CCFE
CULHAM CENTRE FOR
FUSION ENERGY

UK Atomic
Energy
Authority

UKAEA-CCFE-CP(19)34

Jean-Christophe Sublet, Mark R. Gilbert

NEUTRON-INDUCED DAMAGE SIMULATIONS: NOVEL NUCLEAR DATA FORMS AND METRICS FOR MATERIAL SCIENCES

NEUTRON-INDUCED DAMAGE SIMULATIONS: NOVEL NUCLEAR DATA FORMS AND METRICS FOR MATERIAL SCIENCES

Jean-Christophe Sublet, Mark R. Gilbert

NEUTRON-INDUCED DAMAGE SIMULATIONS: NOVEL NUCLEAR DATA FORMS AND METRICS FOR MATERIAL SCIENCES

Jean-Christophe Sublet[1] **and Mark R. Gilbert**[2]
[1]International Atomic Energy Agency
Wagramerstrasse 5, 1400 Vienna, Austria

[2]United Kingdom Atomic Energy Authority
Culham Science Centre, Abingdon OX14 3DB, UK

j.c.sublet@iaea.org, mark.gilbert@ukaea.uk

ABSTRACT

Nuclear interactions can be the source of atomic displacement, embrittlement and post-short-term cascade annealing defects in irradiated structural materials. Such metrics are derived from, or can be correlated to, nuclear kinematic simulations of primary atomic energy distributions spectra and the quantification of the numbers of secondary defects produced per primary as a function of the available recoils, residual and emitted, energies and spectra. Recoils kinematics of neutral, residual, charged and also now including multi-particle emissions occurring at high MeV range energy are more rigorously treated when based on modern, complete and enhanced nuclear data parsed in state of the art processing tools. Examples using the latest processing protocols and metrics applied on recently released TENDL-2017, ENDF/B-VIII and JENDL-4 are given, while novel approaches are proposed.

KEYWORDS: Damage Energy, Defect Production Cross Section, Displacement Per Atom, Recoil Kinematics, Material Sciences

1. INTRODUCTION

Defect production metrics are the starting point in the complex problem of simulating but also correlating the behaviour of materials under irradiation, as direct measurements are extremely difficult and improbable. The multi-scale dimensions (nuclear-atomic-molecular-material) of the simulation processes is tackled from the Fermi gradation to provide the atomic- and meso-scale dimensions with better metrics relying upon a deeper understanding and modelling capabilities at the nuclear level. Detailed, segregated primary knock-on-atom metrics are now available as the starting point of further simulation processes of isolated and/or clustered phenomena in material lattices. This new framework permits more materials, incident energy ranges and particles, irradiations conditions to be explored, when sufficient data exists, to more robustly cover the novel applications: advanced-fission, accelerators, nuclear medicine, space and fusion.

2. Processing protocols: Kerma, Damage Energy, Gas Production

Novel data forms for the 83 naturally occurring elements (assembled from their isotopic parts that in fine will compose the alloy) that include total and partial neutron induced defect production, gas production cross section and kerma factors have been systematically and uniformly derived from the latest ENDF/B-VIII.0, JENDL-4.0 and TENDL-2017 files using the HEATR and GASPR [1,2,3] module protocols of the most recent NJOY2016 release. Building from the information contained in the original isotopic evaluation, the HEATR module computes the heating kerma and the radiation damage energy production; the latter using the Lindhard electronic screening damage function with a displacement threshold relating to the element (although applied to all isotopes) usually comprised between 25 and 90 eV. Below this threshold the traditional Norgett-Robinson-Torrens (NRT) [4,5] damage metric does not apply. The numerous open channels are usually lumped into macro ones mostly relating to neutron transport theory: total, elastic scattering, total inelastic and neutron disappearance. Such an arrangement is valid in the low energy range, below the MeV range, but it does not properly account for the more complex high-energy events, that require multi-body kinematics to be considered.

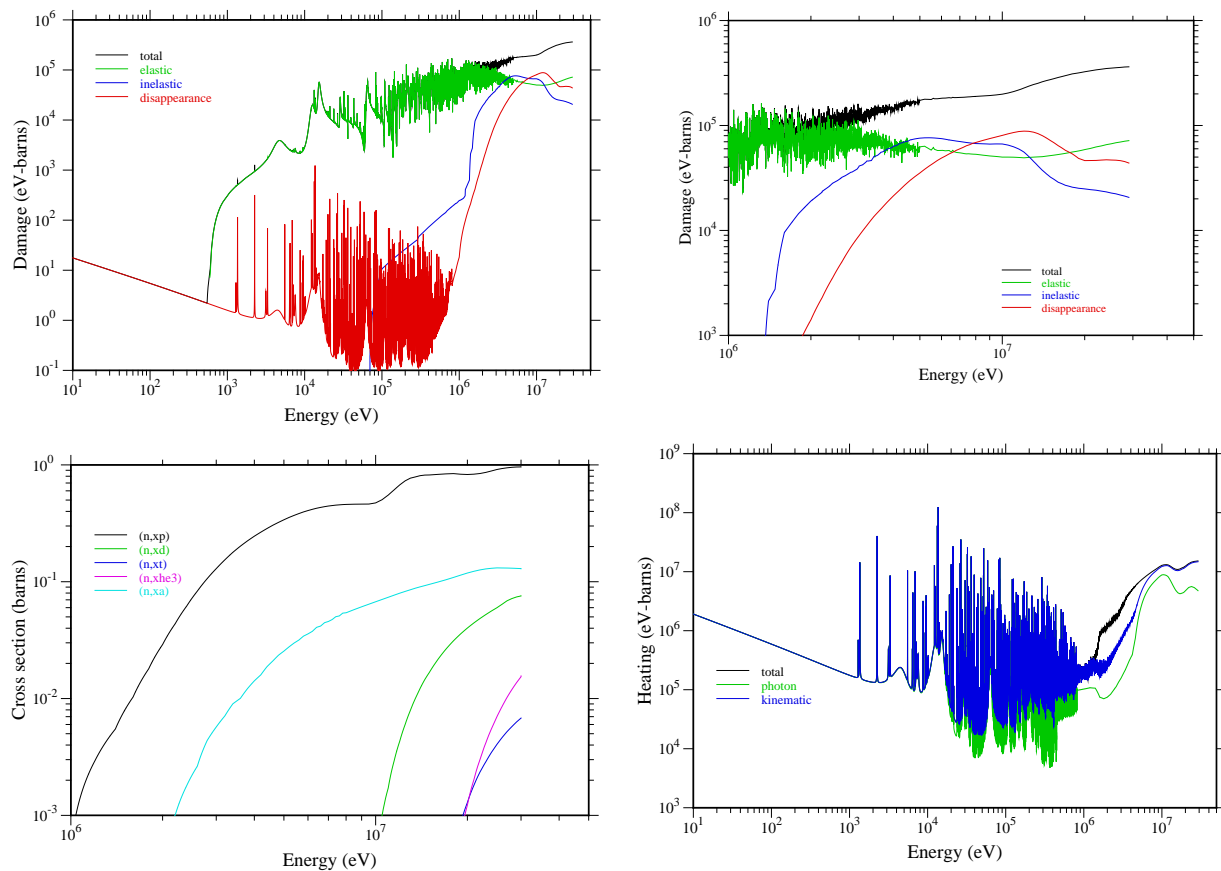

Figure 1: Top defect production cross section. Bottom left gas production cross section. Bottom right prompt kinetic energy release using the energy balance method, kinematic limit is also shown in blue; all derived forms based on TENDL-2017

To add total gas production the GASPR module is used to evaluate and sum-up all channels that would lead to one or more of ^{1}H, ^{2}H, ^{3}H, ^{3}He or ^{4}He emitted particles. It is worth noticing at that stage that GASPR does not account for when the residual is one of these particles as a result of a direct interaction or break-up. Such added complexity is usually handled through properly conducted inventory simulations that account for all decay processes and only really noticeable in light target nuclei. Note that gas production can vary widely depending on which library it stems from, as exemplified by the comparisons in Figure 2.

Figures1 highlights the novel derived, now elemental data forms, clearly showing the complex energy dependence of those metrics, encompassing at the same time the isotopic but also summed channels aspects. When focusing on the damage energy metric, it is clear that above the MeV level other non-scattering, neutron disappearance events start playing a much more important role. The possibility that these multi-body, transmuted residual events might be responsible for anomalous damage phenomena is not often considered within materials modelling frameworks.
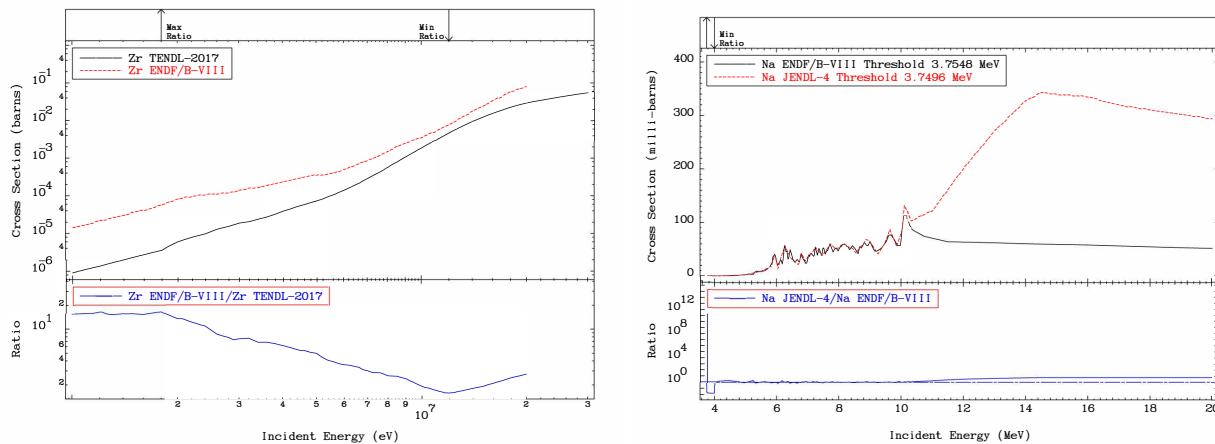

Figure 2: Left Helium production in Zr -TENDL-2017 and ENDF/B-VIII - 60 to 1500%. Right Hydrogen production In Sodium,ENDF/B-VIII and JENDL-4.0

3. Processing protocols: Recoil, Particle Matrices

Another module of NJOY2016, GROUPR [3] has also been used to calculate residual nucleus (A > 4) and emitted particle matrices: energy-angle distribution, exemplified in Figure 3. The group-to-group matrices are computed for every secondary particles and residual nucleus. This processing contrasts with the neutron-gamma only production matrices needed for transport simulations. The GROUPR module has built-in logic to automatically recognise the need to either access the distribution from File 4 (angle only) or File 6 (energy-angle). Each channel cross section group constant is taken at 293.6K for every channel (or MT reaction number) of the File 3 on a fine group structure: 660 groups evenly distributed with 50 bins per decade. It is not uncommon in modern evaluation to have to account for above 50 residual recoils matrices with neutron incident energy up to 30 MeV. The uniformity of the structure but also the detail they now convey allows a much better insight into the data involved. For continuum center of mass distributions in File 6, the

low-energy shape should go like $\sqrt{E}$. However, many library evaluations for File 6 are prepared using advanced model codes: GNASH or TALYS. These model codes naturally produce spectra represented with histogram bins, so giving a constant probability from "zero" ($1.0\,10^{-5}$ eV) energy to the first bin boundary (in those codes), around the keV level. This first histogram bin grossly overestimates the energy shape. The version of GROUPR [3] used here has default coding that replaces the coarse histogram with a finer one that represent the $\sqrt{E}$ shape more closely. This novel feature clearly shows in Figure 4 in the low energy tails of the spectra of Na and Mg for Al irradiation.

This methodology is crucial to provide better, more detailed metrics, energy-dependant recoil atom and emitted particle spectra for material science applications. SPECTRA-PKA applications library files covering all 287 stable isotopic targets, derived from TENDL-2017, JENDL-4.0 and ENDF/B-VIII.0 have now been made available [6].
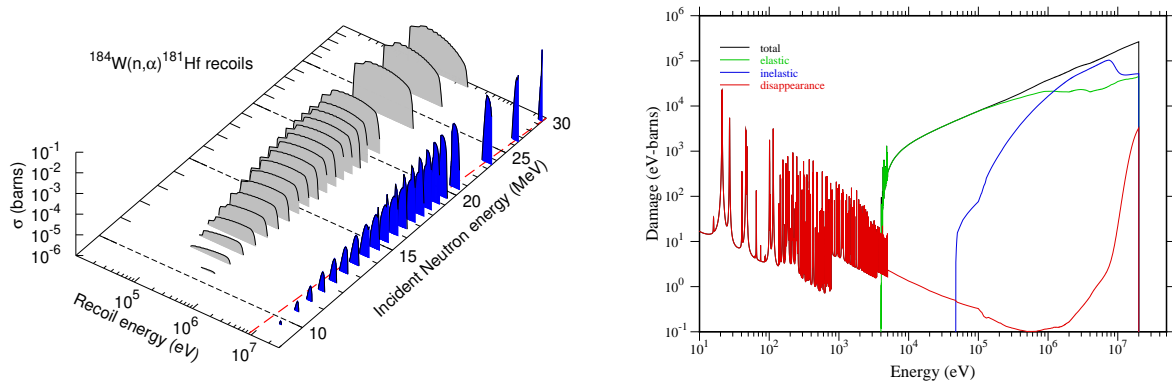

Figure 3: **Left positive Q (+7.3 MeV) (n,α) on ^{184}W recoil distributions, separated for the residual ^{181}Hf (grey), and emitted ^{4}He (blue). The red line represents the energy at which the recoil energy is equal to the incident neutron energy, demonstrating that the emitted particle energies are higher than the incoming neutron because of the positive Q value; Right JENDL-4 W elemental damage energy cross section, the red resonant profile pertaining to the (n,α) channel**

4. Damage Metrics

The recently developed and released SPECTRA-PKA [7,9,10,8] code reads-in the aforementioned recoil matrices and combines these with an incident neutron energy spectrum to define PKA event and energy distributions. The code has the advantage of being fully compatible with the latest modern nuclear data libraries, for both neutron and charge particles, and can handle fine group structures. The code can also consider any complex material composition containing an arbitrary distribution of target nuclide species. Even more significantly, it treats every nuclear reaction channel (on every target nuclide considered), and its associated recoil matrix, separately, which allows a deeper interrogation of the underlying nuclear data.

Figures 4 show examples of the detailed output afforded by the approach taken by SPECTRA-PKA. The left graph shows the elemental (and emitted secondary light gas particle) contributions to the PKAs produced in pure aluminium under a fusion neutron irradiation field. As would be predicted, recoils of Al dominate and are mainly caused by simple scattering events on the target
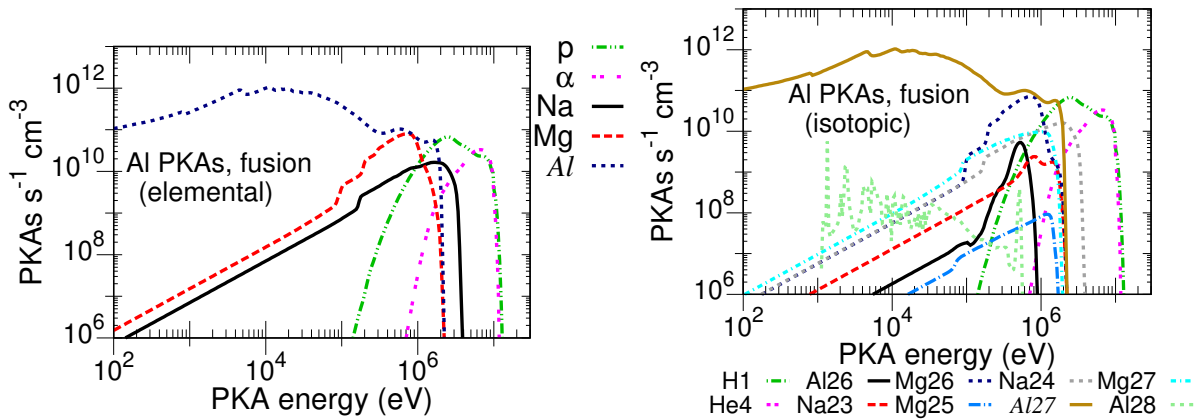
Figure 4: **Pure aluminium (100% ^{27}Al) transmuted residual elements and emitted particle PKA distributions under fusion neutron conditions, right elemental, left isotopic**

^{27}Al atoms. However, there are significant PKA distributions of Mg and Na, as well as from light alpha (^{4}He) particles and protons (^{1}H), which originate from more exotic reactions, such as (n,α) and (n,p). This capability (to separate contributions due to different reaction types) is a powerful unique feature of SPECTRA-PKA and offers future compatibility with advanced materials modelling efforts, where the impact of damage cascades initiated by foreign atomic species introduced into a host lattice can be accounted for. Figure 4 right graph shows the additional complexity even further, by separating out the contributions to the elemental PKA distributions of Al from the different nuclides, showing, for example, that the Al distribution in fig. 4 left is actually the sum of PKA distributions of ^{27}Al, ^{26}Al, and ^{28}Al.

From a material modelling perspective a more important metric than the raw PKA flux-energy distributions are the cumulative probability distributions of PKAs, which give an indication of the relative contributions from different PKA energies. Such cumulative curves (exemplified in figure 5) can be directly used in statistical or Monte Carlo modelling of damage creation and evolution [7].

4.1. Novel Metrics: Damage Energy Per Channel

More recently the per-channel capabilities of SPECTRA-PKA have been exploited to analyze the relative significance of different nuclide channels to dpa damage production rates. For example, Figure 6 shows the dpa-rate contributions in pure nickel under two different neutron irradiation scenarios. The plot includes results from recoil matrices extracted by NJOY2016 from evaluated data forms using the recently released TENDL-2017 and ENDF/B-VIII.0 nuclear data libraries. Figure 6a shows results under typical pressurized water fission reactor (PWR) conditions – in this case the fuel assembly-averaged spectrum for the type P4 pressurized-water reactor at the Paluel site in France – and Figure 6b shows the dpa breakdown under the predicted conditions in the plasma-exposed first wall of a conceptual design for a fusion power plant.

The first noteworthy point in the Figure is the absence of dpa contributions in either plot from
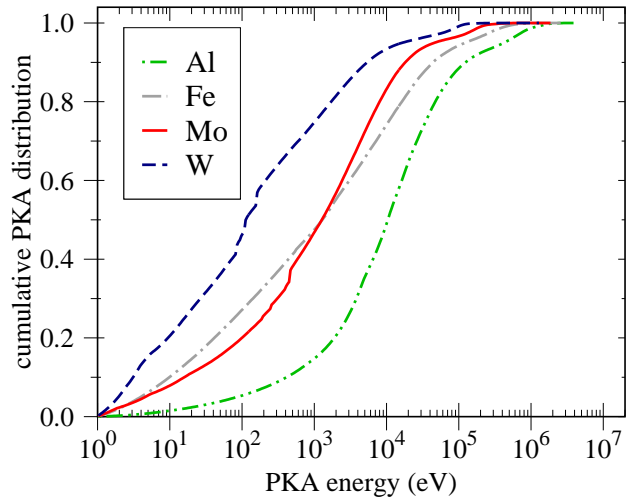
Figure 5: Cumulative probability distribution of PKAs in several different elements under a fusion neutron irradiation spectrum.

nonelastic reactions when using the ENDF/B-VIII.0 library, leading to an underestimation in the total dpa rates relative to TENDL-2017. For example, the ENDF/B-VIII.0 library predicts only 6 dpa/year under fusion DEMO conditions, while TENDL-2017 predicts more than 11. This is due to the absence of the appropriate nuclear data forms (recoils, and particle spectra-angular distributions) in the data-blocks of the ENDF-6 formatted files used to represent the nuclear data in this libraries. Such finding is not isolated, even for an element as important as Ni that could be considered as well known and validated because present in several operational nuclear application.

Another interesting difference between the two sets of results, and one that the advanced features of SPECTRA-PKA are able to highlight, is the change in the proportion of the dpa coming from different reaction channels. In the fission case (Figure6a) scattering (elastic and inelastic scattering have been combined in the plots) makes up more than 90% of the total dpa rate and there are only minor contributions from nonelastic reactions such as (n,p) and (n,α). Under fusion conditions, on the other hand, scattering only accounts for around 61% of the dpa (the % contributions to the total in the TENDL-2017 case are given above each bar) – note that ENDF/B-VIII.0 and TENDL-2017 agree well in their predictions of the dpa contribution from scattering, but ENDF/B-VIII.0 misses the remainder. This highlight the fact that not all, even been recognised, nuclear data library are able to satisfy all application needs.

Figure 7 left demonstrates another important capability of PKA evaluation, namely the ability to consider complex material compositions. Of course, this is standard in many nuclear analysis codes for inventory, burn-up or transport calculations, but SPECTRA-PKA can consider damage contributions (PKAs and dpa) for any distribution of nuclides in the same per-reaction-channel framework. The Figure shows the dpa contributions to 316 stainless steel under PWR conditions. In this case the complexity is illustrated by considering the dpa contributions as a function of reaction-daughters under the hypothesis that the way damage will be created will vary according to the elemental species forming the PKA.
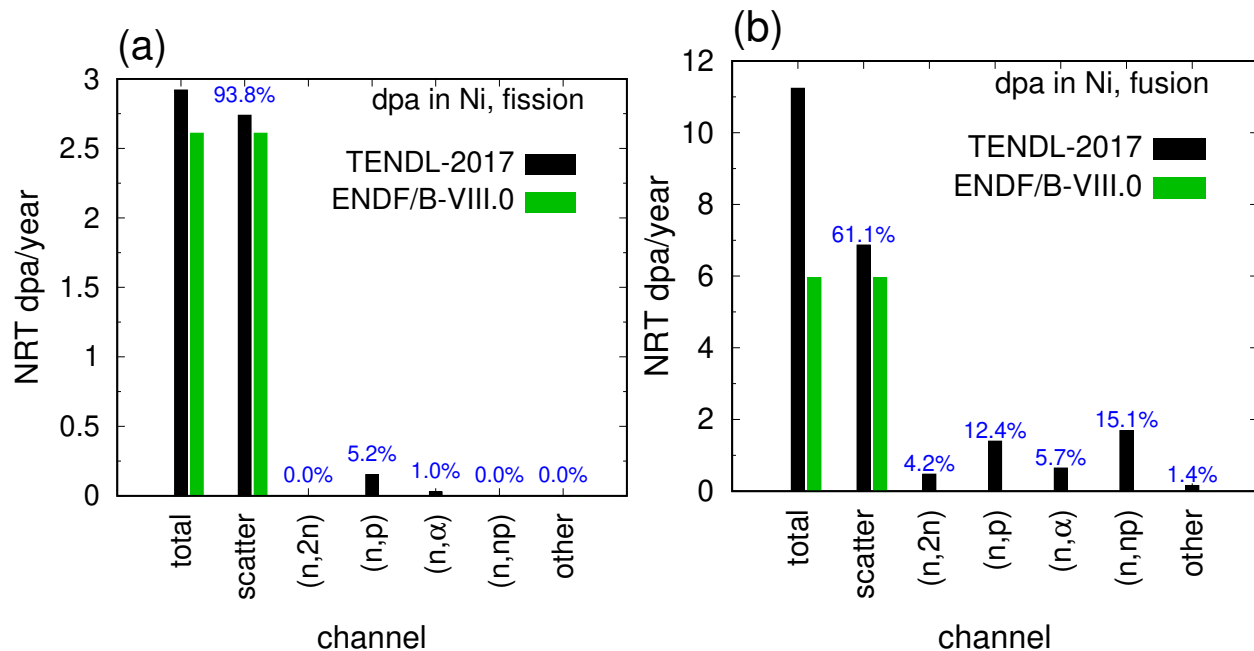
Figure 6: dpa contributions to the total damage rate in pure Ni under (a) typical PWR (fuel assembly average) and (b) typical fusion power plant first wall conditions. Results are given for evaluations using two different nuclear data libraries.

4.1.1. Damage Energy from Decay Events

An additional highlight from the SPECTRA-PKA framework is the consideration of the contribution to displacement events from decay events. Under irradiation it was shown that the extra recoils from the decaying residuals generated by transmutation were not a significant contributor to the overall PKA rates. However, these "decay-recoils" will continue to be present even after the irradiation has terminated, and will then be the only source of displacement damage events (potentially for many years). Figure 7 right, compares the approximate decay-recoil contributions (points) to the curves of neutron-induced PKA distributions in tungsten after 1-year of irradiation. Note that the elemental picture of the PKAs from the neutron irradiation field at t=1-year (the curves shown in the figure) is quite different to the picture at t=0 because of the growth of transmutation elements (Re, Os, Ta,..) in such a material. These transmutant PKA contributions are additionally joined by the set of point PKA-rate approximations from the various decay-species in the composition at this time.

5. CONCLUSIONS

Within the SPECTRA-PKA framework, when fed with proper data forms: residual nucleus (A>4) and emitted particle (A<4) matrices: energy-angle distribution derived from ENDF/B-VIII.0, JENDL-4.0 and TENDL-2017; it is now possible to better simulate, gain insight across the nuclear landscape with the aim of safely, and robustly and scientifically answer the needs of materials science. In comparison to what was available previously the now fully isotopic nuclear libraries
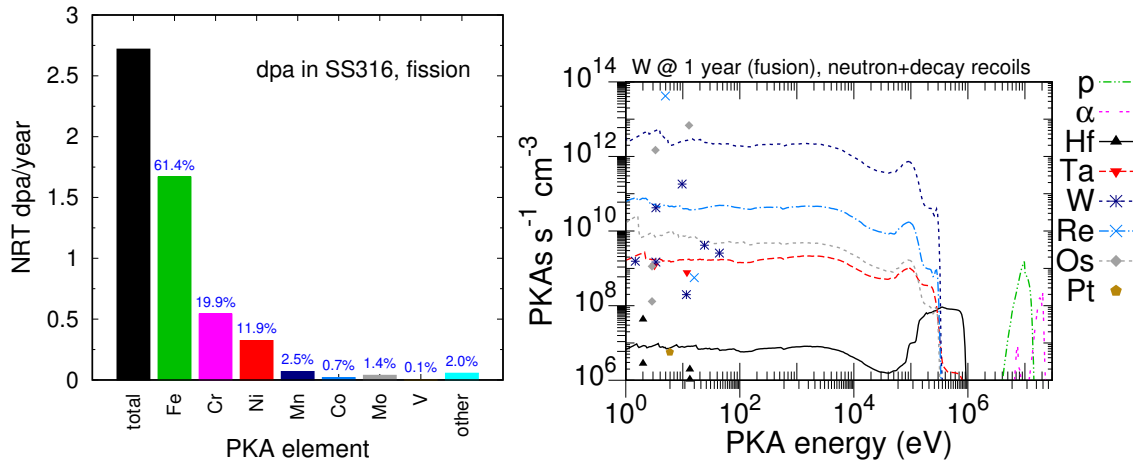
Figure 7: Left dpa contributions to the total damage rate in SS316 steel under PWR conditions, Right PKA contributions from both transmutant/descendant elements (curves) and decaying species (points) to the PKA distributions in pure tungsten after a 1-year irradiation in a typical fusion neutron field

account for: the "minor, lesse" isotopes (e.g. ^{54}Fe, ^{59}Ni, ^{13}C,..) that have subtle effect on the elemental data; the above MeV range multi-body events; and complete angular-energy distribution for all bodies including residual and emitted. With clear, understood processing protocols and pathways that are able to assemble the required elemental data forms, multi-scale simulations can rely on robust foundation from which to deploy modelling and correlation of radiation damage in different challenging environments. With the computational power now available one may even contemplate the deployment of uncertainty propagation, if available within the nuclear data sources.

REFERENCES

[1] R.E. MacFarlane, D. W. Muir and F. M. Mann, "Radiation Damage Calculations With NJOY," J. NUCL. MATER. **122-123**, 1041-46 (1984).

[2] R.E. MacFarlane and A.C. Kahler, "Methods for processing ENDF/B-VII with NJOY," NUCL. DATA SHEETS **111**, 2739 (2010).

[3] R. E. MacFarlane, D. W. Muir, R. M. Boicourt, A. C. Kahler, J. L. Conlin, and W. Haeck. "The NJOY nuclear data processing system, version 2016,". Los Alamos National Laboratory LA-UR-17-20093 (2016). https://www.njoy21.io/NJOY2016/.

[4] M. J. Norgett, M. T. Robinson, and I. M. Torrens, "A proposed method of calculating displacement dose rates," NUCL. ENG. DES. **33**, 50–54 (1975).

[5] G. R. Odette and D. R. Doiron, "Neutron-Energy-Dependent Defect Production Cross Sections for Fission and Fusion Applications," NUCL. TECH. **29**, 346–367 (1976).

[6] "FISPACT-II, Nuclear Data", (2018) https://fispact.ukaea.uk/nuclear-data/.

[7] M. R. Gilbert, J. Marian, J. -Ch. Sublet, Energy spectra of primary knock-on atoms under neutron irradiation, *J. Nucl. Mater* **467**, 121–134 (2015). `doi:https://doi.org/10.1016/j.jnucmat.2015.09.023`.

[8] M. R. Gilbert, SPECTRA-PKA, SPECTRA-PKA is available as a utility within FISPACT-II, and now also available to download from github at https://github.com/fispact/SPECTRA-PKA (2018).

[9] M. R. Gilbert, J.-Ch. Sublet, PKA distributions: Contributions from transmutation products and from radioactive decay, *Nucl. Mater. Energy* **9**, 576–580 (2016). `doi:http://dx.doi.org/10.1016/j.nme.2016.02.006`.

[10] M. R. Gilbert, J.-Ch. Sublet, Differential dpa calculations with SPECTRA-PKA, *J. Nucl. Mater* **504**, 101–108 (2018). `doi:https://doi.org/10.1016/j.jnucmat.2018.03.032`.